High Resolution Beacon-based Proximity Detection for Dense Deployment

Pai Chet Ng, James She, *Member, IEEE* and Soochang Park, *Member, IEEE*

Abstract—The emergence of Bluetooth low energy (BLE) beacons has promoted the development of proximity-based service (PBS), which is a context-aware application delivered subject to the Proximity of Interest (PoI). Most commercial applications use the sequential proximity detection with a fixed scanning mechanism to identify the target PoI. Such sequential execution, though is able to produce reliable detection, suffers severe performance degradation especially when the number of deployed beacons in the vicinity increases. To understand the effects of dense deployment, we conduct an empirical investigation and derive the statistical properties of both received signal strength (RSS) and signal inter-arrival time. In light of the statistical insights, this paper proposes a high resolution proximity detection using an adaptive scanning mechanism fusion with a spontaneous Differential Evolution (*AS+sDE*). This novel approach enables the receiver to adapt its scanning duration conditioned on the deployment density and make an almost spontaneous detection in parallel with the scanning. The feasibility of the proposed approach is verified by both simulations and real-world implementations. For a density of $\leq 5\, beacons/m^2$, *AS+sDE* achieves a superior performance with a high accuracy rate, i.e., on average $< 1s$ is spent to guarantee at least 90% accuracy.

Index Terms—Proximity detection, Bluetooth Low Energy Beacon, Proximity-based Services, Deployment density

1 Introduction

Large scale wireless network deployment, especially the mobile ad-hoc network via Bluetooth Low Energy (BLE) beacons [1] [2], has inspired diverse context-aware applications (e.g., [3] [4] [5] [6]), which can be broadly classified into the following two types: location-based services (LBSs) and proximity-based services (PBSs). In general, both LBSs and PBSs might use similar infrastructures; however, the underlying operational logics are different. An LBS is a location-restricted service delivered according to the location information [7] [8] [9], which can be estimated via the received signal strength (RSS)-based localization techniques, such as trilateration [10] [11] and fingerprinting [12] [13] [14]. A PBS, on the other hand, delivers the context-aware services according to the proximity between a receiving node (RN) and a Proximity of Interest (PoI), regardless of the exact location of the RN [15] [16]. The notion of the PoI is defined to refer to an object or a location that is designated to deliver a specific PBS to the encountered RN, and the proximity detection refers to the technique in detecting the target PoI. Similar to the RSS-based localization techniques [17] [18], most proximity detection techniques exploit the RSS measurements to detect the target PoI [19] [20].

In recent years, the wide accessibility of Bluetooth technology in off-the-shelf smartphones has made BLE beacons one of the best infrastructures for the PBS developments [21] [22]. In fact, most BLE beacons on the market now, e.g., iBeacon by Apple[1], Eddystone by Google[2] and AltBeacon by Radius Networks[3], are directed at the PBS developments. Often, an open-source software development kit (SDK) are provided freely by these manufacturers to fasten the development cycle. In general, beacon-based proximity detection is computationally inexpensive,in addition to the strong technical supports from the mobile development community. Such promise has promoted the development of PBS-related applications such as proximity marketing [23] [24], presence tracking [25] [26] [27], occupancy detection [28] [29], proximity authentication [30] [31], proximity-based multimedia content sharing [32] [33], proximity-based guidance for the blind [34], etc.

Clearly, the active involvement of these industries has contributed to the exponential growth of PBS-related applications on the commercial market. Such growth has led to a massive deployment of beacons in the public spaces such as airports, shopping malls, museums, etc. While many are excited by the unlimited business opportunities with the PBS systems based on BLE beacon technology, little attention has been devoted to exploring the possible challenges with regard to such massive deployment. Furthermore, current beacon-based proximity detection can only achieve up to room level accuracy [35] [36]. In other words, the detection performance will be severely affected when there are more than two PoIs to be detected in a given room. That is to say, the room level accuracy might fail to satisfy the detection performance required by a PBS system, given the increasing number of PoIs within a small area.

Most commercial PBS systems use the provided SDKs to develop their applications. These SDKs mostly employ the sequential proximity detection with a fixed scanning (*FS*) mechanism; the RN is initiated to scan for any observable

• *P.C. Ng, J. She and S. Park are with the Department of Electronic and Computer Engineering, Hong Kong University of Science and Technology. E-mail: pcng@ust.hk, eejames@ust.hk, eewinter@ust.hk*

Manuscript received mm dd, yyyy; revised mm dd, yyyy.

1. "iBeacon for Developers", "https://developer.apple.com/ibeacon/"
2. "Eddystone", "https://developers.google.com/beacons"
3. "AltBeacon: The Open and Interoperable Proximity Beacon", "http://altbeacon.org/"

This article has been accepted for publication in a future issue of this journal, but has not been fully edited. Content may change prior to final publication. Citation information: DOI 10.1109/TMC.2017.2759734, IEEE Transactions on Mobile Computing

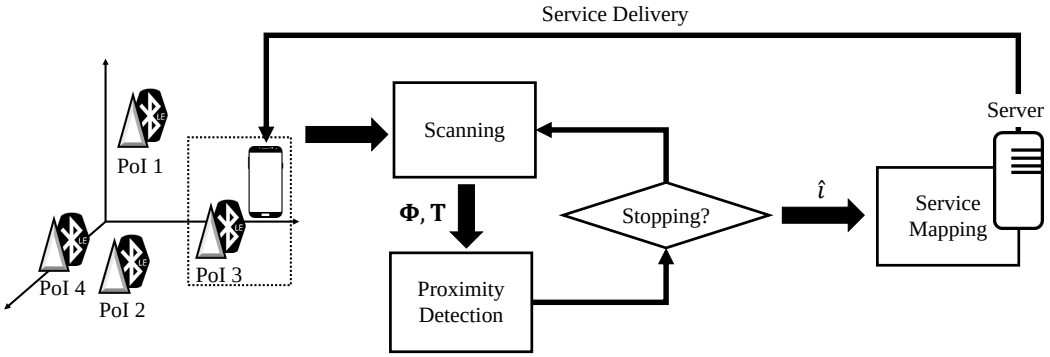

Fig. 1. The proposed approach uses an adaptive scanning fusion with a spontaneous differential evolution to achieve a better proximity detection.

beacon signals, identify the target PoI based on the collected signals and output the detection decision to the server for service mapping. In general, *FS* is able to return an accurate detection when there are only a few deployed beacons with sufficient separation distance. However, such an approach might suffer severe performance degradation when the density of the beacon deployment in the vicinity increases, not to mention the narrow channel width allocated for each beacon signal (i.e., 2MHz), which further increases the chances of signal collision [37].

To address the above issues, a thorough empirical investigation is conducted to analyze the statistical properties of beacon signals in the vicinity with dense deployment. Inspired by the insights acquired from the empirical analysis, this paper proposes a novel adaptive scanning mechanism fusion with a spontaneous Differential Evolution (*AS+sDE*). As illustrated in Fig. 1, instead of sequentially execute the long scanning follows by the proximity detection; the proposed approach uses a very short scanning duration to achieve a seemingly parallel proximity detection. The stopping condition is used to check if an optimal detection decision is achieved, and to adapt the scanning duration if otherwise. The main contributions of this paper are as follows:

1) *Statistical Properties of Beacon Signals*: We verify the RSS distribution with a set of real experimental beacon signals and derive the signal inter-arrival time based on the empirical observation.
2) *Adaptive Scanning fusion with Spontaneous Differential Evolution*: As opposed to the sequential scanning, processing and decision making, the proposed approach processes the signals and makes a spontaneous detection in parallel with the scanning conditioned on the deployment density.
3) *Detection Accuracy and Accuracy rate*: We adopt the conventional probability measure to evaluate the detection accuracy, and further refine the performance measure by confining the accuracy to response time.
4) *Simulation and Practical Experiment*: Based on the derived statistical properties, a simulation program is built to benchmark the performance of the proposed approach with other commonly used approaches. The feasibility of the proposed approach is further verified by real-world implementations.

The rest of the paper is organized as follows. Section 2 describes the two main operations in a beacon-based PBS system. Section 3 derives the statistical properties of beacon signals according to the empirical observation. Section 4 presents the proposed approach, i.e., (*AS+sDE*). Section 5 describes the simulation environment and presents the results. In this section, two performance measures, i.e., the detection accuracy (A_D) and the detection rate (A_r) are described to evaluate the detection performance. Section 6 illustrates the real-world implementations and discusses the results. Section 7 concludes the paper.

2 Beacon-based PBS System

A PBS system is defined as a particular region that provides specified context-aware service. In particular, the system leverages the BLE beacons as the basic infrastructures to interact with the RN before delivering the service. BLE can be configured into four device roles: peripheral, central, broadcaster and observer (refers to [38] for detailed descriptions on each device role). The role of interest in this paper is either the peripheral or broadcaster, which is widely known as BLE beacon. A BLE beacon advertises its signals periodically according to a pre-configured advertising interval T_a, which defines the frequency of the beacon signals being transmitted for a given duration. Given T_a, the number of signals which can be observed by an RN in $1\,s$ is

$$\mathcal{N}_f = \frac{1}{T_a}, \quad (signals/s), \tag{1}$$

where $\mathcal{N}_f$ is the expected number of observable signals per second, and T_a typically ranges from $20\,ms$ to $20\,s$ subject to the beacon configuration. Clearly, the number of signals that can be observed by an RN increases with decreasing T_a. Even though a high $\mathcal{N}_f$ can help the RN in making a correct detection, a short T_a, however, can be a threat to the beacon's battery life.

The fundamental infrastructure of a beacon-based PBS system is the deployed BLE beacons, and we denote an object or a location that is associated with a beacon as the Proximity of Interest (PoI). Mathematically, the PoI in a PBS system can be expressed by a set of vectors/matrices:

$$\mathbf{\Omega} = \{\mathbf{\Omega_b} : b = \{1, 2, ..., N\}\}, \tag{2}$$

where b is a set of indexes denoting a particular *PoI*. Each vector Ω_b can be characterized by its features such as

TABLE 1
Related variables and their notations

Variable	Notation
Advertising interval	T_a
Scanning duration	T_s
Expected number of observable signals in $1\,s$	$\mathcal{N}_f$
Total number of observable signals in T_s	K
A PoI representation in a PBS system	$\mathbf{\Omega_b}$
A set of PoI's indexes	b
Total number of PoIs for a PBS system	N
Signal arrival rate	λ
Beacon to receiving node distance	d_{br}
Deployment density	D
Coverage area of a PBS system	A
Time average RSS from the ith PoI	ϕ_i
Average inter-arrival time for the signals from the ith PoI	τ_i
Energy level contributed by the ith PoI	E_i
Instantaneous RSS in the unit of $Watt$	$P_{r,Watt}$
Instantaneous RSS in the unit of dBm	$P_{r,dBm}$

RSS, time of arrival (ToA), etc. In this paper, we use the instantaneous RSS measurements and the inter-arrival time to characterize the PoI.

Each PoI in a PBS system is designed to serve the same PBS but with a different context; for example, a restaurant establishes a food ordering PBS system by associating a beacon to each dining table. In this case, each dining table is a PoI that serves the same food ordering service but each table has their own unique meta-context such as the table number, virtual robot servant, etc. Other examples include the logistic management in the warehouses and the luggage tracking in the airports.

Obviously, there should not be any issues when there is only one PoI for the entire PBS system; however, many real-world implementations often require more than one PoI to achieve the ultimate objective of their application design. The challenges arise when the number of PoIs required in the vicinity increases. The following subsections describe two main operations dealing with a beacon-based PBS system, i.e., the scanning and the proximity detection. To facilitate the rest of the discussion, we summarize all the relevant notations in Table 1.

2.1 Scanning

As discussed, the two features of interest which can be used to represent a PoI are the received signal strength (RSS) and the signal inter-arrival time. RSS describes the log-ratio of the received power (in $milliWatt$) to the referenced power at $1\,mW$ [39], i.e.,

$$P_{r,dBm} = 10 \log \frac{P_{r,Watt}}{1\,mW}, \tag{3}$$

where $P_{r,dBm}$ is the RSS measurement in dBm, and $P_{r,Watt}$ is the instantaneous signal power in $Watt$.

Before an RN can measure any incoming signals, it must first initiate the scanning. Instead of scan continuously, most RNs are configured to have a fixed scanning duration T_s. In general, T_s must be at least two times greater than T_a to ensure a high signal acquisition rate. When T_s is shorter than T_a, the likelihood for the RN of seeing a signal is relatively low.

Now, suppose that T_s is longer than T_a and multiple RSS measurements are observed by the RN, i.e., $\mathbf{P_{r,dBm}} = \{P_{r,dBm}(t_k) : 0 < k < K \vee t_k \leq T_s\}$, then for a given T_s, the time average RSS from the ith beacon can be computed as follows:

$$\phi_i = \frac{1}{K} \sum_{k=1}^{K} P^{(i)}_{r,dBm}(t_k), \qquad \forall i \in b, \tag{4}$$

where t_k denotes the kth discrete time a beacon signal is observed for $k = (0, K]$ and K is the total number of signals observed during T_s, which according to Eq. (1), should be $K \leq \mathcal{N}_f \times T_s$. In particular, t_1 is the time when the beacon signal first arrived at the RN, t_2 is the time for the second arrival and t_k is the time for the kth arrival. Hence, the average inter-arrival time between the k and $k-1$ observed signals can be described as follows:

$$\tau_i = \begin{cases} \frac{1}{k-1} \sum_{k=2}^{K} (t_k - t_{k-1}), & \text{if } k \geq 3 \\ t_k - t_{k-1}, & \text{if } k = 2 \\ t_k, & \text{if } k = 1 \\ 0, & \text{if } k = 0 \end{cases}, \qquad \forall i \in b, \tag{5}$$

In most cases, we exclude the arrival time at $k = 1$ from the average calculation as the time for the first arrival is random, and the RN might receive the first signal immediately if the RN initiates the scanning right after the next signal transmission. Section 3 further discusses the effect of the distance between the RN and the beacon on the inter-arrival time based on the empirical observation.

Since a PBS system normally consists of more than one PoI and assuming that each beacon associated with each PoI functions perfectly, then all the ϕ_i and τ_i registered by the RN given a certain scanning duration can be described with the following two n dimensional observed vectors,

$$\mathbf{\Phi} = \begin{pmatrix} \phi_1 \\ \vdots \\ \phi_n \end{pmatrix}, \qquad \mathbf{T} = \begin{pmatrix} \tau_1 \\ \vdots \\ \tau_n \end{pmatrix}, \tag{6}$$

where ϕ_1 and τ_1 are the time average RSS and the inter-arrival time representation of PoI 1, respectively, i.e., $\mathbf{\Omega_1} = \{\phi_1, \tau_1\}$, $\mathbf{\Omega_2} = \{\phi_2, \tau_2\}$ and so on. n is the total number of PoIs seen by the RN in the current scanning. Note that n does not necessarily represent the total number of PoIs, and the value of n might differ for each scanning. In other words, not all the PoIs are observed during a scanning unless $n = N$, where N is the total number of PoIs for a PBS system.

This article has been accepted for publication in a future issue of this journal, but has not been fully edited. Content may change prior to final publication. Citation information: DOI 10.1109/TMC.2017.2759734, IEEE Transactions on Mobile Computing

Since T_s for most RNs are fixed, the underlying question here is what should be the best configuration of T_s such that the RN can see all the N beacons signals? Furthermore, how can we still guarantee a good detection performance in the vicinity with dense deployment? The RN might unable to make a correct judgment and thus return an incorrect detection when it fails to observe the complete picture of a PBS system. More specifically, an incorrect detection decision will be produced when there are insufficient number of RSS measurements for the RN to vote. The situation get even more complicated when the RSS contributed by the adjacent PoIs exhibit a almost similar distribution and confuse the RN. To understand the relationship between the observed vectors with respect to the scanning duration and the deployment density, Section 3 provides an empirical analysis based on the real experimental beacons signals and derives their statistical properties.

2.2 Proximity Detection

As illustrated in Fig. 1, the next operation following the scanning is the proximity detection. Proximity detection identifies the target PoI based on the observed vectors. Here, we consider the two observed vectors as described in Eq. (6). Suppose that there are in total N number of PoIs for a PBS system, after the scanning, n number of time average RSSs and inter-arrival times are observed, then based on these observed vectors, we can calculate the energy level as follows:

$$\mathbf{E} = \mathbf{\Psi}^T \mathbf{T}, \tag{7}$$

where the observed vector $\mathbf{T} \in \mathbb{R}^n$ consists of the inter-arrival times from n number of PoIs, and $\mathbf{\Psi} \in \mathbb{R}^n$ is the vector of the time average RSS in the $Watt$ scale obtained through the following conversion:

$$\mathbf{\Psi} = 10^{-3} \times 10^{\frac{\mathbf{\Phi}}{10}} = 10^{-3+\frac{\mathbf{\Phi}}{10}}. \tag{8}$$

Based on the resultant energy level vector $\mathbf{E} \in \mathbb{R}^n$, we can identify the target PoI by taking the entry that returns the highest energy level. The intuition here is that the target PoI where the RN is currently in proximity with should produce the highest energy level. Hence, the proximity detection model can be formulated as follows:

$$\widehat{i} := \underset{i \in b_n}{\arg\max}\{E_i\}. \tag{9}$$

where E_i is the energy level for PoI_i, b_n is the reduced set of the PoI's indexes subject to the n number of PoIs observed during T_s, and $b_n \subseteq b$.

Once the index of the target PoI $\widehat{i}$ is identified, the RN forwards the detection output to the server to request the mapped service. Clearly an incorrect detection will eventually lead to an incorrect PBS delivery, it is thus important to have a reliable proximity detection. To improve the detection performance, one can increase the length of T_s such that the RN can acquire a better picture regarding the number of PoIs in a PBS system. However, searching over all the elements in $\mathbf{E}$ can be a lengthy process. Nonetheless, there are still possibilities to miss the target signal even with such a long T_s. Such a scenario gets even worse when the deployment density increases. Before furthering the discussion on our proposed approach in Section 4, the next section presents an empirical analysis based on the real RSS measurements, which provides the insight towards the design of the proposed approach.

Fig. 2. The setting of (a) experiment 1 to investigate the effect of d_{br}, and (b) experiment 2 to investigate the effect of D.

3 Empirical Analysis

Suppose that all the deployed beacons are configured to have the same T_a, the time for an RN to observe the first signal is still random due to the following reasons. First, the time for each beacon to start their transmission is random; and second, some signals might get attenuated or collided along their propagation path. The time for a signal to arrive at the RN is further subject to the distance between the beacon and the RN. Since signals are susceptible to environmental noise, the chances of them being attenuated before reaching the RN increases with increasing distance. Given a short T_s, the RN might fail to observe a complete picture regarding all the PoIs in a PBS system as a consequence of the aforementioned scenarios. Furthermore, signal collision is unavoidable when there are many PoIs in the vicinity. In other words, dense deployment might further shrink the size of the observed vectors (i.e., $\mathbf{\Phi}$ and $\mathbf{T}$) due to the signal collisions.

Consider the two parameters, i.e., distance and density, which might affect the complete observation at the RN, we set up two experiments as depicted in Fig. 2 to examine the effect of (a) the distance between the beacon and the RN d_{br}, and (b) the deployment density D. Experiment 1 was conducted in a long corridor with a single beacon, in total 1000 RSS measurements were collected from $0\,m$ to $10\,m$ with $1\,m$ increment every step. Experiment 2 was conducted in a small classroom by varying the number of beacons from 1 to 12. Similarly, 1000 signals samples were collected before increasing the number of beacons. The empirical analysis of each experiment is presented in Section 3.1 and Section 3.2, respectively.

3.1 Beacon to Receiver Node Distance

Fig. 3(a) depicts the RSS variation with respect to time when the receiver was placed $10\,m$ from the beacon. It can be observed that even though the RSS fluctuates over time, the

This article has been accepted for publication in a future issue of this journal, but has not been fully edited. Content may change prior to final publication. Citation information: DOI 10.1109/TMC.2017.2759734, IEEE Transactions on Mobile Computing

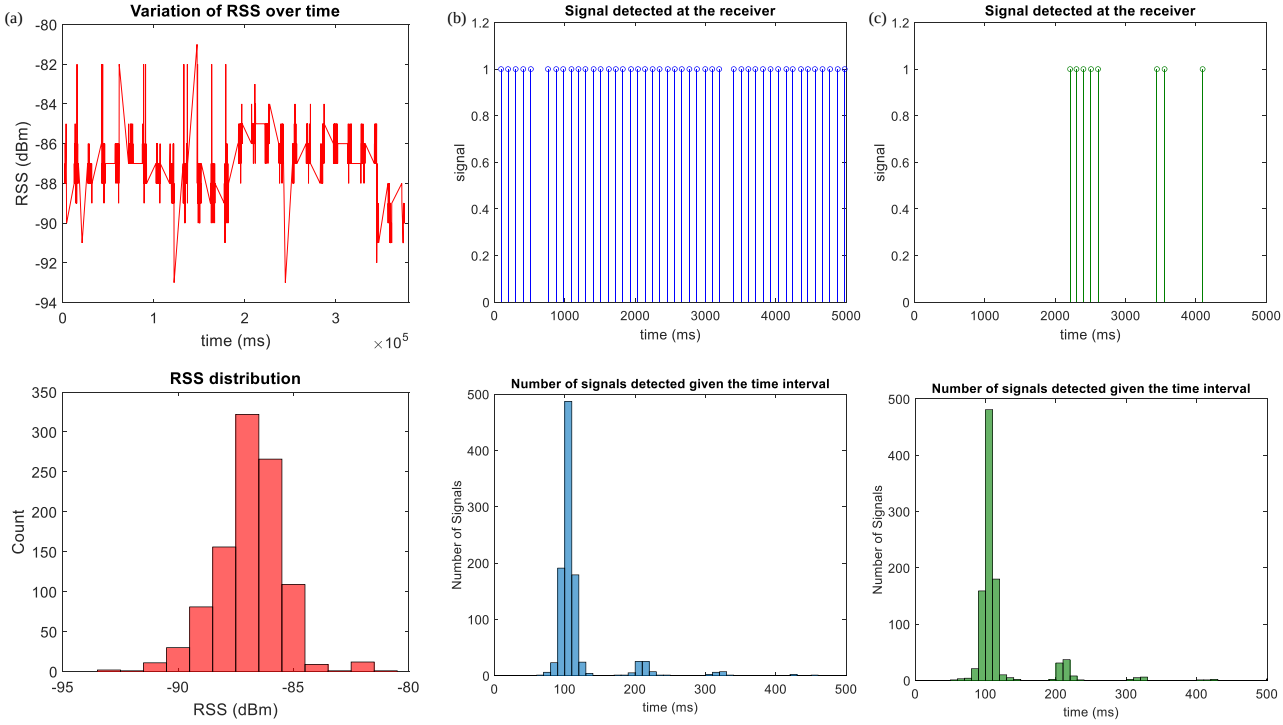

Fig. 3. The empirical observations based on: (a) the RSS variation and their distribution with $d_{br} = 10\,m$; and (b) and (c) the signal inter-arrival process with $d_{br} = 2\,m$ and $d_{br} = 10\,m$, respectively.

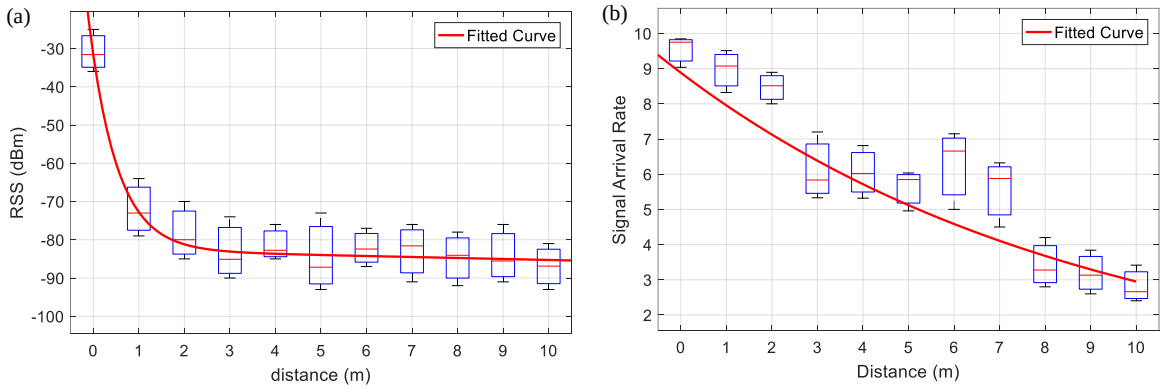

Fig. 4. Least square fitting is used to find the relationship: (a) between the measured RSS and actual distance, and (b) between the signal arrival rate and the actual distance.

fluctuation indeed follows a Gaussian distribution, as stated in [40],

$$f_{\phi}(P_{r,dBm}(t)) = \frac{1}{\sigma\sqrt{2\pi}} \exp\left(-\frac{1}{2}(\frac{P_{r,dBm}(t)-\phi}{\sigma})^2\right), \tag{10}$$

where ϕ and σ^2 are the mean and the variance, respectively, calculated with respect to the distance, d_{br}. The effects of d_{br} on the RSS fluctuation for d_{br} ranging from $1\,m$ to $10\,m$ are plotted in Fig. 4(a), and the least square fitting method is used to find the best fit curve. It can be observed that the fitted curve follows the general path loss model [41], which can be described by the following equation:

$$P_{r,dBm} = \alpha 10^{d_{br}} + \beta, \tag{11}$$

where α is a constant and β is the corresponding loss exponent induced by the surrounding noise.

The signal arrival patterns and their inter-arrival distribution with $d_{br} = 2\,m$ and $d_{br} = 10\,m$ are illustrated in Fig. 3(b) and (c), respectively. It can be observed that the signal inter-arrival time follows a Poisson arrival process, with the arrival rate varying according to d_{br}. In other words, signals take a longer time to arrive at the RN when d_{br} increases. By distributing the signal inter-arrival time conditioned on the number of received signals, the Poisson arrival process can be described by the following equation:

$$f_{\tau}(\tau|K) = \exp(-\lambda t)\frac{\lambda^K}{K!}, \tag{12}$$

where λ is the signal arrival rate and K is the total number of signals observed during T_s.

Eq. (12) clearly tells that the signal inter-arrival time depends on the signal arrival rate λ. If T_a is set to $100\,ms$,

This article has been accepted for publication in a future issue of this journal, but has not been fully edited. Content may change prior to final publication. Citation information: DOI 10.1109/TMC.2017.2759734, IEEE Transactions on Mobile Computing

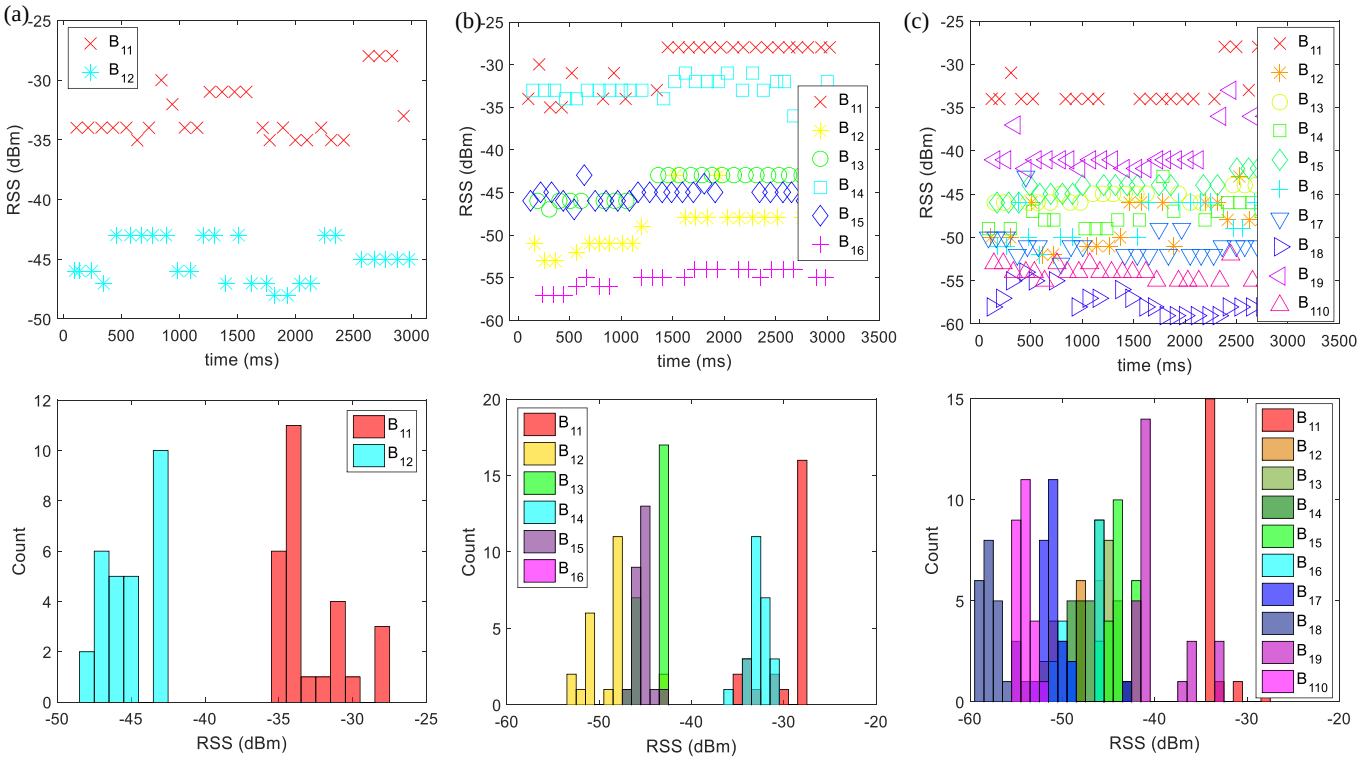

Fig. 5. The distribution of RSS when the beacon density equals to (a) $2\,beacons/m^2$, (b) $6\,beacons/m^2$ and (c)$10\,beacons/m^2$.

then according to Eq. (1), the total expected number of arrival signals in $1s$ should be 10. However, in a practical scenario, the actual signal arrival rate, λ_{actual}, is generally less than $\mathcal{N}_f$, and λ_{actual} decreases with increasing d_{br}. To understand the relationship between λ_{actual} and d_{br}, the signal arrival rates at different distances are calculated and the resultant data points are plotted, as shown in Fig. 4(b). Similarly, the least square fitting method is used, and the corresponding best fit equation is obtained as follow:

$$\lambda_{actual} = \frac{1}{T_a}\exp(-T_a d_{br}). \tag{13}$$

From Eq. (13), it is clear that λ_{actual} depends on the beacon advertising interval, T_a. The maximum λ_{actual} is around 9 at a distance $\leq 1\,m$, this shows that most signals are able to reach the RN successfully when d_{br} is small. In other words, the RN needs to have a longer T_s to guarantee no signals are missed when d_{br} increases.

3.2 Signal Properties in a Dense Beacon Network

Given the total area covering a PBS system, the deployment density can be defined as follows:

$$D = \frac{N}{A}, \quad (beacons/m^2), \tag{14}$$

where N denotes the total number of PoIs in the vicinity and A is the total coverage area of a PBS system.

Fig. 5 illustrates the mutual interference between neighboring beacons, with D equal to $2\,beacons/m^2$, $6\,beacons/m^2$ and $10\,beacons/m^2$. When $D = 2\,beacons/m^2$, the signals are still distinguishable, but when D continues to increase, e.g., $D = 10\,beacons/m^2$,

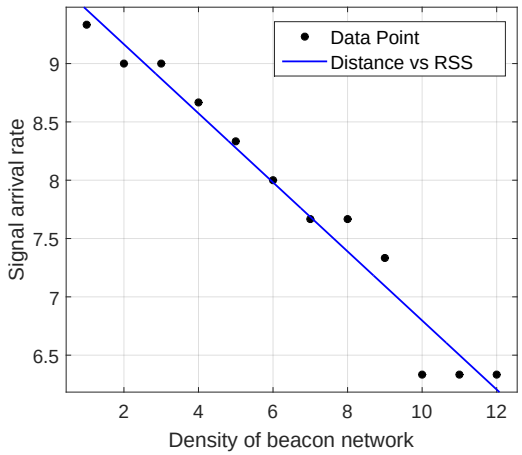

Fig. 6. The setting of (a) experiment 1 to investigate the effect of d_{br}, and (b) experiment 2 to investigate the effect of D.

the RN might find it difficult to distinguish the signals and thus identify the target PoI. Moreover, every beacon in the vicinity continuously advertises their signals independently according to their own pre-defined T_a, collision problem arises when D increases. Such collision further affects the signal arrival rate. The relationship between λ and D is plotted in Fig. 6, which can be expressed as follows:

$$\lambda = -\gamma D + \lambda_{actual}, \tag{15}$$

where γ is the decaying constant and λ_{actual} is the actual signal arrival rate.

From the empirical analysis, it is clear that both d_{br} and D affect the RSS variation and the inter-arrival time. This simply implies that the conventional scanning mechanism relying on a fixed T_s is most likely to produce an incorrect detection output when either D or d_{br} increase. Even though increasing T_s can achieve a more complete signal acquisition regarding the deployed PBS system, a long T_s might, in turn, prolong the service delivery and eventually affect users' experiences. In other words, a good beacon-based PBS system should be able to deliver a correct service within an acceptable delivery time. A correct service delivered beyond an acceptable time can have a negative impact on the users' experiences.

4 Proposed Solution

As discussed in Section 1, the conventional sequential execution employed by most PBS systems simply scan for a fixed duration T_s and then select the target PoI based on the observed vector. This, though able to detect the target PoI provided T_s is sufficiently long and D is low, suffers from performance degradation when D increases. Furthermore, the RN will continue to scan until it completes the scanning cycle despite the fact that the signal from the target PoI has been received.

In view of the inflexibility of the conventional approach, this paper proposes a novel proximity detection approach by adapting a scanning duration in parallel with a spontaneous Differential Evolution (*AS+sDE*), as illustrated in Fig. 1. Instead of scanning for a fixed and long T_s, the proposed approach uses a very short T_s to enable the system in making an almost spontaneous detection output seemingly in parallel with the scanning. The stopping conditions are introduced for two purposes: to adapt the scanning duration, and to determine the final detection output. The adaptive scanning and the detection output based on the spontaneous differential evolution are discussed in Section 4.1 and Section 4.2, respectively.

4.1 Adaptive Scanning Mechanism

During the scanning, the RN is able to listen to any incoming signals in the vicinity. The beacon density for some PBS systems might not necessarily remain the same thorough the time. The changing density is an unavoidable scenario for certain PBS-related use cases, for example, the logistic management in the warehouses or the luggage tracking in the airports. The intense shipping activities in the warehouses will change the density from time to time. Nowadays a lot of airports had started to offer beacon association to the luggage. The beacon density for a given luggage arrival track is always varying, subject to the arrival and departure of the luggage. Even though the beacon density for a restaurant use case is fairly fixed, the restaurant might also experience a certain change in the beacon density when extra dining table is added or a few tables are merged to serve a bigger group.

The unpredictable density changes further affect the detection performance of the conventional scanning mechanism in which the fixed T_s might unable to capture adequate number of signal samples for decision making and thus producing an incorrect detection output. Such an incorrect detection can be avoided if the RN is capable of adapting its T_s conditioned to the changing density. The algorithm of the adaptive scanning (*AS*) mechanism is described as follows:

Algorithm 1 Adaptive Scanning (*AS*)

Input : $T_s = \tilde{t}$, $maxIter = 100$
Output: Observed vectors, $\tilde{\mathbf{\Phi}}$ and $\tilde{\mathbf{T}}$
Initialize: $count = size(\tilde{\mathbf{\Phi}})$, $iter = 1$, $compareRatio = 0$

while $t < T_s$ **do**
  if $iter == 1$ **then**
    Store and average:
     - the instantaneous $P_{r,dBm}$ into $\tilde{\mathbf{\Phi}}$
     - the inter-arrival time into $\tilde{\mathbf{T}}$
  else if $iter \geq 1$ **then**
    Store and average:
     - the instantaneous $P_{r,dBm}$ into $\tilde{\mathbf{\Phi}}^{(iter)}$
     - the inter-arrival time into $\tilde{\mathbf{T}}^{(iter)}$
  else if $iter \geq 2$ **then**
    Compare $\tilde{\mathbf{\Phi}}^{(iter-1)}$ and $\tilde{\mathbf{T}}^{(iter-1)}$
     with $\tilde{\mathbf{\Phi}}^{(iter)}$ and $\tilde{\mathbf{T}}^{(iter)}$
     and update the $\tilde{\mathbf{\Phi}}$ and $\tilde{\mathbf{T}}$
     Set $compareRatio = \frac{size(\tilde{\mathbf{\Phi}}^{(iter-1)})}{size(\tilde{\mathbf{\Phi}}^{(iter)})}$
  else
    Increase $iter$ by 1
  end
  if *count* ≥ 3 *or* $compareRatio == 1$ *or* $iter > maxIter$ **then**
    Forward the current $\tilde{\mathbf{\Phi}}$ and $\tilde{\mathbf{T}}$ to the *sDE* function
     BREAK and exit the **WHILE** loop
  end
end

As illustrated in **Algorithm 1**, the RN first initiates $T_s = \tilde{t}$. In general, $\tilde{t}$ is set to equal to T_a because the likelihood of seeing a signal is relatively low when $T_s < T_a$. In case the T_a is unknown to the RN, the RN can first scan continuously until the first signal is received, and then estimates the T_a from the first received signal. Mathematically, $\tilde{t}$ can be estimated as follows:

$$\tilde{t} = \begin{cases} T_a, & \text{if } T_a \text{ is known} \\ 2 \times t_k, & \text{if } T_a \text{ is unknown} \\ \mathcal{S} \times \tilde{t}, & \text{if } \mathcal{S} \text{ is available} \end{cases}, \tag{16}$$

where $\mathcal{S}$ is a tuning parameter produced by *sDE* from time to time and $\mathcal{S} = (0, 2]$.

Even though it is a common practice to set a same T_a for all the beacons, some PBS systems might use a different T_a for different beacons to suit their application requirement. For example, the PBS systems which prioritizing the service according to the user's group or imposing different interactivity elements at different PoIs. In this case, we still can set the T_s to the first T_a estimated from the system and then adjust the $\tilde{t}$ from time to time according to $\mathcal{S}$ produced by *sDE*, which is discussed in the next section. The idea is just to make sure the RN is able to observe some signals during the scanning rather than enforcing the RN to a particular T_s. In general, it is desirable to have the scanning duration as

short as possible such that the RN can detect the target PoI spontaneously using the extended differential evolution.

Within the *while* loop, the RN will check if at least three different sets of signals (i.e., from different beacons) are received; if yes, the RN will pause its current scan and proceed to *sDE* to identify the temporary detection output. Such a condition is set because the minimum number of signals required by *sDE* is 3. The detailed descriptions of *sDE* are presented in the next subsection. Besides this *while* conditional statement, there are another two *if* conditional statements. The first *if* statement compares the elements in the current observed vectors with the previous observed vectors to check if there are any signals from new beacons; if no new set of signal is observed, the RN will terminate its scan and proceed with *sDE*. The second *if* statement checks if the number of iterations reaches the predefined maximum iteration threshold. Such a condition is necessary to avoid the RN being trapped inside the *while* loop.

4.2 Spontaneous Differential Evolution

Differential evolution (*DE*) is a heuristic algorithm which is able to search for an optimum solution that changes over time [42]. Even though *DE* might not always converge to the absolute optimum, it is able to return an approximate optimum solution in a very short time. Most of the proximity/positioning techniques that have adopted the DE algorithm [43] [44] [45], require a large number of RSS measurements before the algorithm can be applied. Such a comprehensive signal acquisition is impractical in a PBS system since near real-time service delivery is expected to ensure the users' experiences.

In contrast, this paper proposes a spontaneous differential evolution (*sDE*) by extending the existing DE such that the proposed *sDE* is able to process the observed vectors almost in parallel with the *AS* mechanism. In general, *sDE* adopts the four fundamental steps described in the legacy *DE* algorithm, i.e., initialization, mutation, recombination and selection.

- *Initialization*: *sDE* initializes the *AS* function and sets the $\tilde{t}$ according to Eq. (16). Once the size of the observed vectors exceeds or equal 3, the scanning is paused immediately. The two observed vectors obtained during the scanning, are forwarded to the *sDE* subroutine. *sDE* sorts the observed vectors in the current generation in descending order. Referring to the observed vectors defined in Eq. (6), the sorted observed vectors can be refined to follow:

$$\tilde{\mathbf{\Phi}}^{(G)} = \left\{ \begin{pmatrix} \phi_1^{(G)} \\ \vdots \\ \phi_{\tilde{n}}^{(G)} \end{pmatrix} : \phi_1^{(G)} > \phi_2^{(G)} > \cdots > \phi_{\tilde{n}}^{(G)} \right\}, \tag{17}$$

$$\tilde{\mathbf{T}}^{(G)} = \left\{ \begin{pmatrix} \tau_1^{(G)} \\ \vdots \\ \tau_{\tilde{n}}^{(G)} \end{pmatrix} : \tau_1^{(G)} > \tau_2^{(G)} > \cdots > \tau_{\tilde{n}}^{(G)} \right\}, \tag{18}$$

where $\tilde{n}$ is the population size of the current generation G, i.e., the total number of PoIs observed in the current scanning. Note that $\tilde{n} \neq n$ and n is generally greater than $\tilde{n}$ in the first few generations; however, as the generation increases, $\tilde{n}$ will eventually be greater than n and approximates N.

- *Mutation*: Two donor vectors are generated based on the top three elements from both $\tilde{\mathbf{\Phi}}^{(G)}$ and $\tilde{\mathbf{T}}^{(G)}$ when $G = 1$; whereas when $G \geq 2$, the donor vectors are calculated based on the top two elements from $\tilde{\mathbf{\Phi}}^{(G)}$ and $\tilde{\mathbf{T}}^{(G)}$ and the selected $\phi_{i_o}^{(G-1)}$ and $\tau_{i_o}^{(G-1)}$. Mathematically, the mutation process between these three elements is formulated as follows:

$$\phi_d^{(G)} = \phi_1^{(G)} + M(\phi_2^{(G)} - \phi_3^{(G)}), \tag{19}$$

$$\tau_d^{(G)} = \tau_1^{(G)} + M(\tau_2^{(G)} - \tau_3^{(G)}), \tag{20}$$

where M is the mutation ratio ranging from $[0, 2]$. $\phi_d^{(G)}$ and $\tau_d^{(G)}$ are the generated donors.

- *Recombination*: Two trials, i.e., $\phi_{\mathbb{T}}^{(G)}$ and $\tau_{\mathbb{T}}^{(G)}$ are produced by combining the two donors with the target elements selected from the previous G. In particular, the target elements ϕ_{i_o} and τ_{i_o} are equal to $\phi_1^{(G)}$ and $\tau_1^{(G)}$ if $G = 1$. If $G > 1$, then the target element is based on the selection output i_o produced by the previous generation $G - 1$. The recombination between the donors and the selected targets is governed by a predefined crossover rate, i.e.,

$$\begin{pmatrix} \phi_{\mathbb{T}}^{(G)} \\ \tau_{\mathbb{T}}^{(G)} \end{pmatrix} = \begin{cases} \begin{pmatrix} \phi_{i_o}^{(G-1)} \\ \tau_{i_o}^{(G-1)} \end{pmatrix}, & \text{if } rand_j \geq C \\ \begin{pmatrix} \phi_d^{(G)} \\ \tau_d^{(G)} \end{pmatrix}, & \text{if } rand_j < C \end{cases}, \tag{21}$$

where the crossover rate C ranges from $(0, 1]$, and $rand_j$ is the random value generated between $[0, 1]$. Note that both M and C are the parameters that introduce certain perturbation to current searching space such that the system is not confine to the initialized searching space and being trapped into current local optimal. While learning the best parameter settings for both M and C are desirable, the learning process indeed take times and large training data is required to achieve the best learning outcome. Consider the real-time requirement of the PBS system, it is impractical to conduct intensive training; hence, in this paper, we did not design the system to learn the optimal parameter settings, instead we manually configure their value according to the suggestion advised in [42]. Future work can be devoted to design a system which is capable of learning the best parameter settings on-the-fly and minimize the required training time to ensure real-time experiences.

- *Selection*: Lastly, the resultant trials ($\phi_{\mathbb{T}}^{(G)}$, $\tau_{\mathbb{T}}^{(G)}$) and the previously selected targets ($\phi_{i_o}^{(G-1)}$, $\tau_{i_o}^{(G-1)}$) are substituted into Eq. (7) to calculate its corresponding signal energy level, i.e.,

$$E_{\mathbb{T}}^{(G)} = \tau_{\mathbb{T}}^{(G)}(10^{-3+\frac{\phi_{\mathbb{T}}^{(G)}}{10}}), \tag{22}$$

$$E_{i_o}^{(G-1)} = \tau_{i_o}^{(G-1)}(10^{-3+\frac{\phi_{i_o}^{(G-1)}}{10}}). \tag{23}$$

With this, the proposed *sDE* only needs to compare the resultant $E_{\mathbb{T}}^{(G)}$ and $E_{i_o}^{(G-1)}$ to select the optimum solution, rather than searching over the entire $\mathbf{E}$ to find the maximum $\widehat{i}$. Note that the selected i_o is just the temporary decision held in the current generation. Mathematically, it can be described as follows:

$$i_o := \underset{i \in b_n}{\arg\max}\{E_{\mathbb{T}}^{(G)}, E_{i_o}^{(G-1)}\}, \tag{24}$$

The temporary selected decision i_o yields another $\phi_{i_o}^{(G)}$ and $\tau_{i_o}^{(G)}$ in the current generation. Besides this, the resultant i_o determines the turning parameter $\mathcal{S}$ for the *AS* process. The turning parameter is set to 1 if $G = 1$; whereas for $G > 1$, the turning parameter can be determined as follows:

$$\mathcal{S} = 2\left(1 - \exp\left(-\frac{E_{i_o}^{(G)}}{E_{i_o}^{(G-1)}}\right)\right). \tag{25}$$

The above equation confines the turning parameter $\mathcal{S}$ to 0 and 2 which satisfies the requirement of Eq. (16). The turning parameter $\mathcal{S}$ is forwarded to the *AS* subroutine to tune the $\tilde{t}$; whereas the resultant $\phi_{i_o}^{(G)}$ and $\tau_{i_o}^{(G)}$ are forwarded to the next generation, and the same procedures are repeated until one of these conditions is met: $\widehat{i}$ converges to a certain value for a consecutive three generations or G reaches the maximum threshold. Upon meeting one of these conditions, the RN stops both *AS* and *sDE* functions simultaneously and set $i_o = \widehat{i}$. The general flow of *sDE* is described in Algorithm 2.

Algorithm 2 Spontaneous Differential Evolution (*sDE*)

Input : Observed vectors, $\tilde{\mathbf{\Phi}}$ and $\tilde{\mathbf{T}}$, $maxG = 100$
Output: Detection output, i_o
Initialize: $population = size(\tilde{\mathbf{\Phi}})$, $G = 1$, $M = 0.8$, $C = 0.5$

Sort both $\tilde{\mathbf{\Phi}}$ and $\tilde{\mathbf{T}}$ in descending order
if $G > 1$ **then**
  Select the top two elements Calculate the turning parameter using Eq. (25)
else
  Select the top three elements Set $\mathcal{S} = 1$
end
Forward the turning parameter to *AS*

Perform:
- mutation using Eq. (19) and (20)
- crossover using Eq. (21)
- selection using Eq. (24)

if $G > 2$ **then**
  if $i_o^{(G-2)} == i_o^{(G-1)} == i_o^{(G)}$ *or* $G > maxG$ **then**
    Set $\widehat{i} = i_o$
    BREAK and exit the **WHILE** loop
  end
end
Increase G by 1

5 Simulation

This section discusses the simulation results obtained from the three approaches, i.e., the fixed scanning mechanism with the maximum selection (*FS+Max*), the adaptive scanning mechanism with the maximum selection (*AS+Max*), and the proposed approach *AS+sDE*. Both *FS+Max* and *AS+Max* are approaches with a sequential execution that performs the scanning, process and detection operations in sequence. Note that even though *AS+Max* employs the adaptive scanning mechanism, a complete signal acquisition are still required before the RN can process the signals, which means the RN needs to repeat its scan until no new signals are observed in the next scanning. However, this is not the case with *AS+sDE* in which the RN can make a spontaneous detection with at least three signal sets, and both *AS* and *sDE* are executed almost in parallel.

Before discussing the simulation environment and the results in Section 5.2 and Section 5.3, respectively, the next subsection first describes the performance measures which are used to benchmark the detection performance.

5.1 Performance Measures

This paper adopts a conventional probability measures to evaluate the detection performance and further refine the adopted measures by taking the response time into consideration. In general, these two performance measures are described as follows:

- *Detection Accuracy*: We adopt the conventional probability measure to evaluate the detection performance by analyzing the number of correct detections with respect to the total number of detections performed by an RN for a given period. In general, the detection accuracy A_D can be expressed as follows:

$$A_D = \frac{1}{N}\sum_{n=1}^{N} O_n, \tag{26}$$

where N is the total number of detections and O_n is the output measured at the nth detection with

$$O = \begin{cases} 1, & \text{if } \widehat{i} = \text{target PoI at } i \\ 0, & \text{if } \widehat{i} \neq \text{target PoI at } i \end{cases}. \tag{27}$$

- *Accuracy Rate*: In fact it is meaningless if the RN needs to take a longer time to achieve a high A_D. Hence, it is vital to examine the total time an RN takes to return the detection output. To investigate the efficiency of the RN in producing a correct detection output with respect to time, we define a performance measure by taking the response time into accuracy consideration. This performance measure is named as accuracy rate A_r, which examines the mean amount of time the RN takes to produce the expected accuracy.

$$A_r = A_D\Big(\sum_{n=1}^{N}\{t_n | O_n = 1\}\Big)^{-1}, \tag{28}$$

where t_n is the total amount of time the RN takes to produce a correct detection, i.e., $O_n = 1$ at the nth detection.

This article has been accepted for publication in a future issue of this journal, but has not been fully edited. Content may change prior to final publication. Citation information: DOI 10.1109/TMC.2017.2759734, IEEE Transactions on Mobile Computing

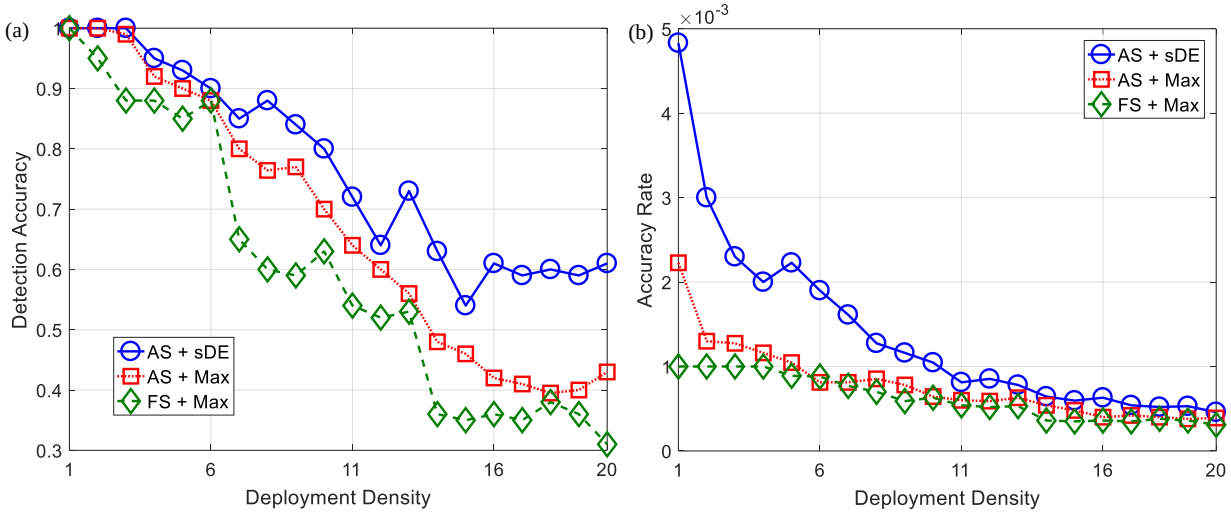

Fig. 7. The simulation compares the results of the three approaches in terms of (a) the detection accuracy, and (b) the accuracy rate with respect to the deployment density.

TABLE 2
Parameter settings for the three simulation environments

Parameter	Horizontal	Vertical	Cube
Area	$2 \times 0.5m^2$	$0.5 \times 2m^2$	$1 \times 1 \times 1m^3$
T_a	100 ms		
Beacon population	1 to 20		
Transmit Power	$0dBm$		
RF channels	Channel 38 ($2474MHz$)		
Carrier frequency	$\pm 150kHz$		

5.2 Simulation Environment

Three types of simulation settings were developed: horizontal, vertical and cube. The horizontal setting aligns the beacons horizontally subject to the total area defined in the simulation. Similarly, the vertical setting aligns the beacons vertically; whereas the cube setting confines the beacons randomly within the enclosed volume. The setting of the related parameters, for these three simulation environments, are summarized in Table 2.

For both the horizontal and vertical settings, the RN is placed at a static point from the beacons. Assume that both x and y coordinate of the ith PoI are known, then the distance between the RN from all the PoIs can be calculated with $d_{xy} = \sqrt{(x_r - x_i)^2 + (y_r - y_i)^2}$. For the cube setting, the PoIs are tabulated around the enclosed volume. For all the simulations, the beacons were set to advertise their signals according to Eq. (10) and (12). In total 100 simulations were executed for each setting, with D increased from $1\,beacons/m^2$ to $20\,beacons/m^2$ with a $1\,beacons/m^2$ increment every step.

5.3 Simulation Results

Both A_D and A_r obtained from all the three settings are averaged and the results are plotted, as shown in Fig. 7(a) and Fig. 7(b), respectively. It is observed that most approaches have a high A_D when D is low, and A_D decreases as D increases. However, *AS+sDE* is able to guarantee an above average detection accuracy (i.e., ≥ 0.5) when D increases beyond $10\,beacons/m^2$. The performance gain is significant comparing to both *AS+Max* and *FS+Max*, in which their detection accuracies drop to below 0.5 when $D > 15\,beacons/m^2$ (for the case of *AS+Max*) and when $D > 14\,beacons/m^2$ (for the case of *FS+Max*). In average, the detection accuracy of *AS+sDE* is approximately 15% higher than both *AS+Max* and *FS+Max*. Such superior performance validates the capability of *AS+sDE* in making a seemingly spontaneous detection while the RN continues to adapt its scanning duration.

Since most PBS systems employ the proximity detection techniques to decide the PoI prior to delivering their services, the total time taken to deliver a service is important to guarantee users' experiences. The detection accuracy conditioned on response time is illustrated in Fig. 7(b). For the *FS+Max* approach, the A_r simply depends on the A_D as T_s is fixed. Obviously, such an approach is simply inflexible as the RN will keep on scan even though the target signal has been received. For example, when $D = 1$, both *AS+Max* and *AS+sDE* are able to return a detection output in less than $1\,s$; however, *FS+Max* still needs to scan for a complete scanning cycle (i.e., $T_s = 1\,s$ in this case) before proceeding with decision making. Further, *AS+sDE* achieves a high A_r at low D and maintains an acceptable A_r when D increases compared to *AS+Max*.

6 Practical Implementation

Three practical PBS systems are implemented to verify the feasibility of the proposed approach. The first implementation is to demonstrate the horizontal setting of a beacon-based PBS system. Note that we did not specify the application purposes but instead implemented a generic system for practical testing in a real testbed. The above setting can be used in many use cases such as student seating, interactive cinema, autonomous restaurant service, etc. The second

This article has been accepted for publication in a future issue of this journal, but has not been fully edited. Content may change prior to final publication. Citation information: DOI 10.1109/TMC.2017.2759734, IEEE Transactions on Mobile Computing

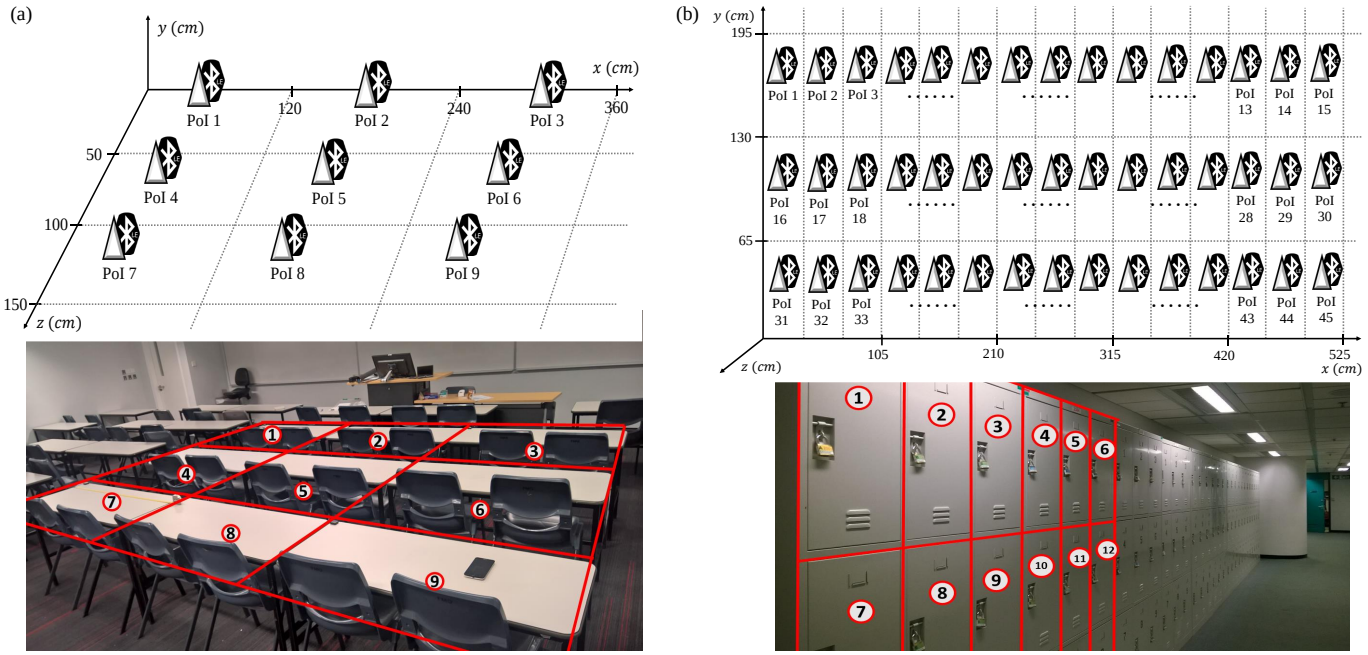

Fig. 8. The experimental testbeds in (a) horizontal setting, and (b) vertical setting.

implementation is set up on the lockers to demonstrate the vertical setting of a beacon-based PBS system. This vertical setting can be applied to various PBS-related use cases such as logistic management, interactive shopping, autonomous library service, etc. The third implementation demonstrates the combination setting of vertical and horizontal alignment.

An Android smartphone, Asus Zenfone 2 Deluxe ZE551ML, was programmed with the three approaches (i.e., *FS+Max*, *AS+Max* and *AS+sDE*) to experiment with both PBS implementations mentioned above. The Apps were written in C#, using Xamarin IDE[4]. In total 9 beacons were used for the first experiment, 45 beacons for the second experiment and 7 beacons for the third experiment. All beacons were built with CC2541 BLE chips from Texas Instrument and powered by CR2450 $3\,V$ lithium coin cell batteries. The transmit power is configured to $0\,dBm$ and operate in the $2.4\,GHz$ ISM band. The next subsection describes the setting of these three experimental testbeds, and follows with a discussion on the experimental results.

6.1 Experimental Testbed

The first testbed was set up in a classroom where a total of 9 beacons were associated with 9 tables, i.e., each table represents a PoI. As illustrated in Fig. 8(a), the total area that covers these 9 PoI is $3.6\,m \times 1.5\,m = 5.4\,m^2$. In other words, the maximum deployment density is approximately $1.67\,beacons/m^2$. This is an acceptable density as according to the simulation results obtained in Fig. 7 in which the three approaches are expected to achieve at least 90% detection accuracy.To verify the results obtained from the simulation, we first experimented on the testbed with only one beacon working in the whole $5.4\,m^2$ area, and slowly increased the number of beacons until all the 9 designated PoIs were associated with a beacon. The experimental results collected from this testbed were analyzed and are presented in the next subsection.

As illustrated in Fig. 8(b), the second testbed demonstrates the vertical setting of a PBS system. In total, 45 beacons were associated with 45 lockers which cover a total area of $5.25\,m \times 1.95\,m = 10.2375\,m^2$. The maximum density for this testbed is approximately $4.4\,beacons/m^2$. Again, referring back to the simulation results shown in Fig. 7, a detection accuracy of more than or equal to 0.8 is expected for all the three approaches.

Fig. 9 depicts the experimental setup for the third implementation – a relaxation zone. This implementation is to demonstrate the combination setting of horizontal and vertical alignment. A total of 7 beacons were associated with 7 different objects/locations enclosed by a $1.5\,m \times 2.1\,m \times 2.4\,m$ space, as illustrated in Fig. 9. The maximum density is approximately $0.9259\,beacons/m^3$, which is equivalent to $2.22\,beacons/m^2$ if all the PoIs are projected onto the $x-z$ plane, $1.39\,beacons/m^2$ onto the $x-y$ plane, or $1.94\,beacons/m^2$ onto the $y-z$ plane. If a worst case is assumed, then, according to Fig. 7, the expected detection accuracy should be at least 0.85 and above. Similarly, the same experimental steps were repeated and the results are discussed in the next subsection.

6.2 Results and Discussion

The results obtained from all three experimental testbeds are plotted in Fig. 10: (a) indicates the results from the classroom, (b) the locker and (c) the relaxation zone. The results show that the A_D for both *AS+Max* and *AS+sDE* are above 0.8 when $D \leq 1\,beacons/m^2$ for all the implementations, which is slightly lower than the A_D obtained from the

4. "Deliver native Android, iOS, and Windows apps, using existing skills, teams, and code.", "https://www.xamarin.com/platform"

This article has been accepted for publication in a future issue of this journal, but has not been fully edited. Content may change prior to final publication. Citation information: DOI 10.1109/TMC.2017.2759734, IEEE Transactions on Mobile Computing

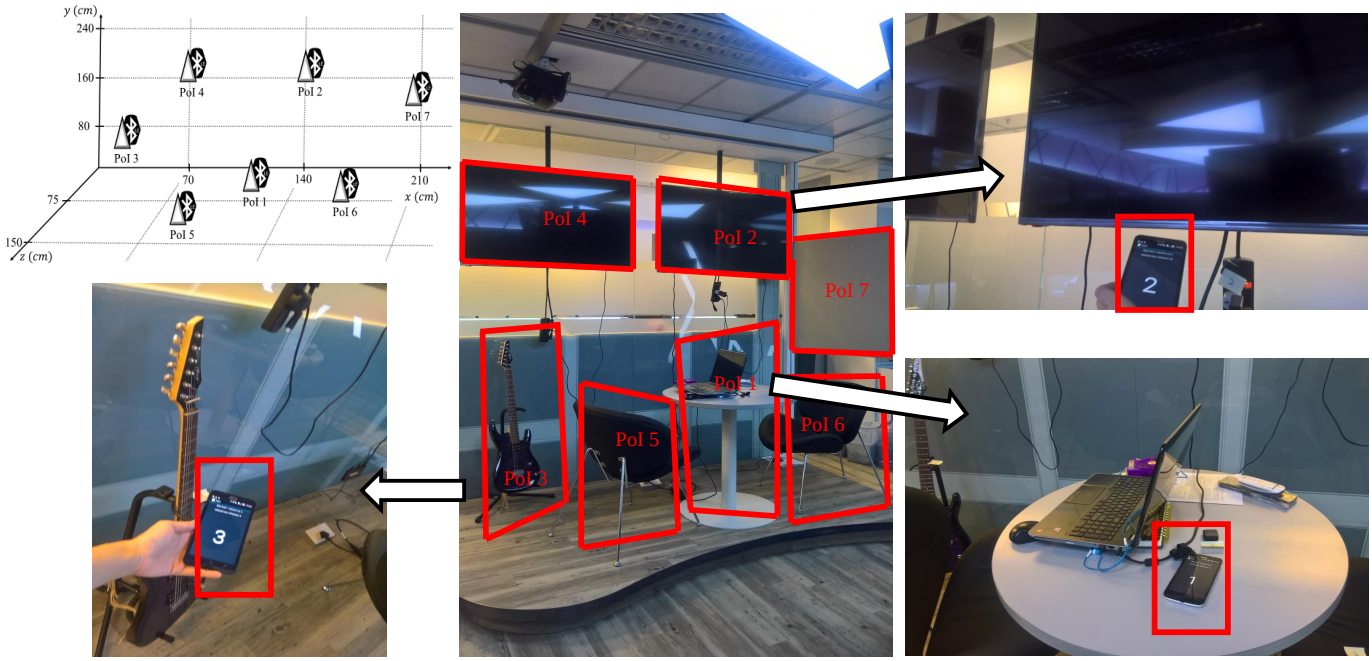

Fig. 9. An experimental testbed with 7 PoIs in a combination of horizontal and vertical setting.

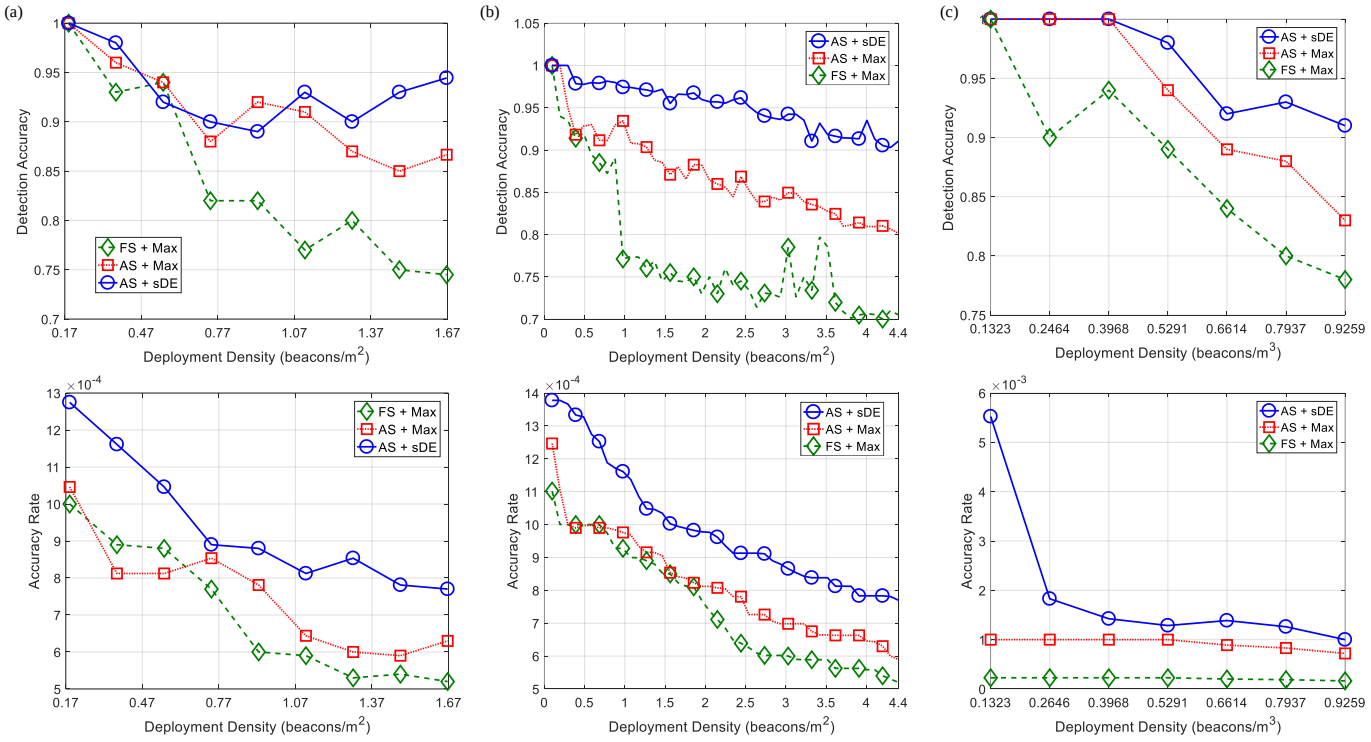

Fig. 10. The detection performance of the three approaches for: (a) the classroom (9 PoIs in a horizontal setting), (b) the locker (45 PoIs in a vertical setting) and (c) the relaxation zone (7 PoIs in a mixed setting).

simulation. However, for *FS+Max* with $T_s = 1\,s$, A_D further drops to below 0.8. As for *AS+sDE*, its detection performance is comparatively more stable, with an average A_D greater than 0.9. Moreover, *AS+sDE* outperforms the other approaches when $D \geq 1\,beacons/m^2$. *AS+sDE* also shows a superior performance in the third implementation when a combination of horizontal and vertical setting is considered. The accuracy rate achieved by *AS+sDE* is always higher than both *AS+Max* and *FS+Max*. This means that *AS+sDE* is not only able to produce high detection accuracy, but the total time it took to return an accurate detection is also fast. This verifies the superiority of *AS+sDE* in executing signal processing and decision making in parallel with the adaptive scanning.

From these three practical implementations, *AS+sDE* further proves its superiority with an average performance gain of 15%. Note that the results obtained from the practical implementations are slightly less than the simulation results (e.g., the simulation results show that A_D should be more than 0.9 when $D < 2\,beacons/m^2$, but the A_D for the practical implementations drop to around 0.8 at the similar density). One possible reason for such a performance degradation is the non-isometric signal coverage of each deployed beacon. Even though beacon signals are assumed to be isometric, such an ideal condition might be forfeited due to the antenna orientation of the deployed beacons, and the presence of obstacles. Additionally, the unexpected environmental noise such as the passing by of nearby people during the experiments causes further signal variation. In particular, the human body is a good absorber of the signals; hence, signal loss rate increases with passers-by and eventually affects the detection performance.

7 Conclusion

This paper proposes a high resolution beacon-based proximity detection using an adaptive scanning mechanism fusion with a spontaneous Differential Evolution (*AS+sDE*) to deliver the proximity-based services (PBSs) in the vicinity with dense deployment. In general, a PBS system delivers context-aware service to the users when they are in close proximity to the Proximity of Interest (PoI). A sequential proximity detection approach with a fixed scanning mechanism, undoubtedly, can return a high detection accuracy when the RN is in the vicinity with sparse deployment. However, a beacon-based PBS system might consist of multiple PoIs with multiple beacons associated with them. Such a scenario complicates the proximity detection and might lead to severe performance degradation if the RN fails to distinguish the signals of the target PoI from the rest of the adjacent PoIs. To address this issue, as well as provide a near real-time detection with high accuracy, this paper proposes *AS+sDE*, which is able to adapt its scanning duration conditioned on the deployment density, and at the same time execute the signal processing and make a spontaneous detection in parallel with the scanning. Both simulations and real-world implementations prove the feasibility of the proposed *AS+sDE*. In addition, *AS+sDE* outperforms the other approaches with a high detection performance, i.e., more than 90% accuracy for a beacon-based PBS system with a density of $< 5\,beacons/m^2$.

Acknowledgments

This work was supported by HKUST-NIE Social Media Laboratory.

References

[1] K.-H. Chang, "Bluetooth: a viable solution for iot?[industry perspectives]," *Wireless Communications, IEEE*, vol. 21, no. 6, pp. 6–7, 2014.

[2] S. Kajioka, T. Mori, T. Uchiya, I. Takumi, and H. Matsuo, "Experiment of indoor position presumption based on rssi of bluetooth le beacon," in *Consumer Electronics (GCCE), 2014 IEEE 3rd Global Conference on*. IEEE, 2014, pp. 337–339.

[3] M. Collotta and G. Pau, "A novel energy management approach for smart homes using bluetooth low energy," *Selected Areas in Communications, IEEE Journal on*, vol. 33, no. 12, pp. 2988–2996, 2015.

[4] M. Choi, W.-K. Park, and I. Lee, "Smart office energy management system using bluetooth low energy based beacons and a mobile app," in *Consumer Electronics (ICCE), 2015 IEEE International Conference on*. IEEE, 2015, pp. 501–502.

[5] A. Beach, M. Gartrell, S. Akkala, J. Elston, J. Kelley, K. Nishimoto, B. Ray, S. Razgulin, K. Sundaresan, B. Surendar *et al.*, "Whozthat? evolving an ecosystem for context-aware mobile social networks," *Network, IEEE*, vol. 22, no. 4, pp. 50–55, 2008.

[6] C. Perera, A. Zaslavsky, P. Christen, and D. Georgakopoulos, "Context aware computing for the internet of things: A survey," *IEEE Communications Surveys Tutorials*, vol. 16, no. 1, pp. 414–454, First 2014.

[7] J. Chon and H. Cha, "Lifemap: A smartphone-based context provider for location-based services," *IEEE Pervasive Computing*, vol. 10, no. 2, pp. 58–67, 2011.

[8] M. Werner, "Indoor location-based services," *Prerequisites and foundations. Cham: Springer*, 2014.

[9] L. Chen, S. Thombre, K. Jrvinen, E. S. Lohan, A. Aln-Savikko, H. Leppkoski, M. Z. H. Bhuiyan, S. Bu-Pasha, G. N. Ferrara, S. Honkala, J. Lindqvist, L. Ruotsalainen, P. Korpisaari, and H. Kuusniemi, "Robustness, security and privacy in location-based services for future iot: A survey," *IEEE Access*, vol. 5, pp. 8956–8977, 2017.

[10] Z. Li, T. Braun, and D. C. Dimitrova, "A passive wifi source localization system based on fine-grained power-based trilateration," in *World of Wireless, Mobile and Multimedia Networks (WoWMoM), 2015 IEEE 16th International Symposium on a*. IEEE, 2015, pp. 1–9.

[11] S. He and S. H. G. Chan, "Intri: Contour-based trilateration for indoor fingerprint-based localization," *IEEE Transactions on Mobile Computing*, vol. 16, no. 6, pp. 1676–1690, June 2017.

[12] L. Chen, L. Pei, H. Kuusniemi, Y. Chen, T. Kröger, and R. Chen, "Bayesian fusion for indoor positioning using bluetooth fingerprints," *Wireless personal communications*, vol. 70, no. 4, pp. 1735–1745, 2013.

[13] F. Palumbo, P. Barsocchi, S. Chessa, and J. C. Augusto, "A stigmergic approach to indoor localization using bluetooth low energy beacons," in *Advanced Video and Signal Based Surveillance (AVSS), 2015 12th IEEE International Conference on*. IEEE, 2015, pp. 1–6.

[14] R. Faragher and R. Harle, "Location fingerprinting with bluetooth low energy beacons," *Selected Areas in Communications, IEEE Journal on*, vol. 33, no. 11, pp. 2418–2428, 2015.

[15] F. Yin, Y. Zhao, F. Gunnarsson, and F. Gustafsson, "Received-signal-strength threshold optimization using gaussian processes," *IEEE Transactions on Signal Processing*, vol. 65, no. 8, pp. 2164–2177, April 2017.

[16] M. M. Scheunemann, K. Dautenhahn, M. Salem, and B. Robins, "Utilizing bluetooth low energy to recognize proximity, touch and humans," in *Robot and Human Interactive Communication (RO-MAN), 2016 25th IEEE International Symposium on*. IEEE, 2016, pp. 362–367.

[17] C. Liu, D. Fang, Z. Yang, H. Jiang, X. Chen, W. Wang, T. Xing, and L. Cai, "Rss distribution-based passive localization and its application in sensor networks," *IEEE Transactions on Wireless Communications*, vol. 15, no. 4, pp. 2883–2895, April 2016.

[18] M. Angjelichinoski, D. Denkovski, V. Atanasovski, and L. Gavrilovska, "Cramér–rao lower bounds of rss-based localization with anchor position uncertainty," *IEEE Transactions on Information Theory*, vol. 61, no. 5, pp. 2807–2834, May 2015.

[19] A. Küpper and G. Treu, "Efficient proximity and separation detection among mobile targets for supporting location-based community services," *ACM SIGMOBILE Mobile Computing and Communications Review*, vol. 10, no. 3, pp. 1–12, 2006.
[20] S. Liu, Y. Jiang, and A. Striegel, "Face-to-face proximity estimationusing bluetooth on smartphones," *Mobile Computing, IEEE Transactions on*, vol. 13, no. 4, pp. 811–823, 2014.
[21] A. Ghose, C. Bhaumik, and T. Chakravarty, "Blueeye: A system for proximity detection using bluetooth on mobile phones," in *Proceedings of the 2013 ACM conference on Pervasive and ubiquitous computing adjunct publication*. ACM, 2013, pp. 1135–1142.
[22] D. Hortelano, T. Olivares, M. C. Ruiz, C. Garrido-Hidalgo, and V. López, "From sensor networks to internet of things. bluetooth low energy, a standard for this evolution," *Sensors*, vol. 17, no. 2, p. 372, 2017.
[23] D. Zaim and M. Bellafkih, "Bluetooth low energy (ble) based geomarketing system," in *2016 11th International Conference on Intelligent Systems: Theories and Applications (SITA)*, Oct 2016, pp. 1–6.
[24] J. Takalo-Mattila, J. Kiljander, and J. P. Soininen, "Advertising semantically described physical items with bluetooth low energy beacons," in *2013 2nd Mediterranean Conference on Embedded Computing (MECO)*, June 2013, pp. 211–214.
[25] Y. Yang, Z. Li, and K. Pahlavan, "Using ibeacon for intelligent in-room presence detection," in *2016 IEEE International Multi-Disciplinary Conference on Cognitive Methods in Situation Awareness and Decision Support (CogSIMA)*, March 2016, pp. 187–191.
[26] A. Alhamoud, A. A. Nair, C. Gottron, D. Bohnstedt, and R. Steinmetz, "Presence detection, identification and tracking in smart homes utilizing bluetooth enabled smartphones," in *Local Computer Networks Workshops (LCN Workshops), 2014 IEEE 39th Conference on*. IEEE, 2014, pp. 784–789.
[27] S. Papaioannou, A. Markham, and N. Trigoni, "Tracking people in highly dynamic industrial environments," *IEEE Transactions on Mobile Computing*.
[28] G. Conte, M. De Marchi, A. A. Nacci, V. Rana, and D. Sciuto, "Bluesentinel: a first approach using ibeacon for an energy efficient occupancy detection system." in *BuildSys@ SenSys*, 2014, pp. 11–19.
[29] A. Filippoupolitis, W. Oliff, and G. Loukas, "Bluetooth low energy based occupancy detection for emergency management," in *2016 15th International Conference on Ubiquitous Computing and Communications and 2016 International Symposium on Cyberspace and Security (IUCC-CSS)*, Dec 2016, pp. 31–38.
[30] M. Portnoi and C.-C. Shen, "Location-aware sign-on and key exchange using attribute-based encryption and bluetooth beacons," in *Communications and Network Security (CNS), 2013 IEEE Conference on*. IEEE, 2013, pp. 405–406.
[31] H. Nakajima, S. Suzuki, T. Tokunaga, K. Tanaka, Y. Miyazaki, K. Maruyama, and O. Nakamura, "Out-of-band authentication protocol for digital signage and smartphone interaction," in *2016 IEEE 5th Global Conference on Consumer Electronics*, Oct 2016, pp. 1–2.
[32] B. Xing, K. Seada, and N. Venkatasubramanian, "Proximiter: Enabling mobile proximity-based content sharing on portable devices," in *Pervasive Computing and Communications, 2009. PerCom 2009. IEEE International Conference on*. IEEE, 2009, pp. 1–3.
[33] C. Shao and S. Nirjon, "Imagebeacon: Broadcasting color images over connectionless bluetooth le packets," in *2017 IEEE/ACM Second International Conference on Internet-of-Things Design and Implementation (IoTDI)*, April 2017, pp. 121–132.
[34] T. Trongwongsa, K. Chankrachang, N. Prompoon, and C. Pattanothai, "Shopping navigation system for visual impaired people based on proximity-based technology," in *Computer Science and Software Engineering (JCSSE), 2015 12th International Joint Conference on*. IEEE, 2015, pp. 263–268.
[35] Y. Agata, J. Hong, and T. Ohtsuki, "Room-level proximity detection using beacon frame from multiple access points," in *2015 Asia-Pacific Signal and Information Processing Association Annual Summit and Conference (APSIPA)*. IEEE, 2015, pp. 941–945.
[36] R. Tabata, A. Hayashi, S. Tokunaga, S. Saiki, M. Nakamura, and S. Matsumoto, "Implementation and evaluation of ble proximity detection mechanism for pass-by framework," in *Computer and Information Science (ICIS), 2016 IEEE/ACIS 15th International Conference on*. IEEE, 2016, pp. 1–6.
[37] M. Wang and J. Brassil, "Managing large scale, ultra-dense beacon deployments in smart campuses," in *Computer Communications Workshops (INFOCOM WKSHPS), 2015 IEEE Conference on*. IEEE, 2015, pp. 606–611.
[38] Bluetooth low energy beacons - texas instruments. [Online]. Available: http://www.ti.com/lit/an/swra475/swra475.pdf
[39] R.-H. Wu, Y.-H. Lee, H.-W. Tseng, Y.-G. Jan, and M.-H. Chuang, "Study of characteristics of rssi signal," in *Industrial Technology, 2008. ICIT 2008. IEEE International Conference on*. IEEE, 2008, pp. 1–3.
[40] C. Feng, W. S. A. Au, S. Valaee, and Z. Tan, "Compressive sensing based positioning using rss of wlan access points," in *INFOCOM, 2010 Proceedings IEEE*. IEEE, 2010, pp. 1–9.
[41] N. Salman, M. Ghogho, and A. H. Kemp, "On the joint estimation of the rss-based location and path-loss exponent," *IEEE Wireless Communications Letters*, vol. 1, no. 1, pp. 34–37, 2012.
[42] R. Storn and K. Price, "Differential evolution–a simple and efficient heuristic for global optimization over continuous spaces," *Journal of global optimization*, vol. 11, no. 4, pp. 341–359, 1997.
[43] A. Masegosa, A. B. E. O. P. Lopez, and G. A. Perallos, "A new optimization approach for indoor location based on differential evolution," 2015.
[44] L. Moreno, S. Garrido, F. Martin, and M. L. Munoz, "Differential evolution approach to the grid-based localization and mapping problem," in *2007 IEEE/RSJ International Conference on Intelligent Robots and Systems*. IEEE, 2007, pp. 3479–3484.
[45] R. Harikrishnan, "An integrated xbee arduino and differential evolution approach for localization in wireless sensor networks," *Procedia Computer Science*, vol. 48, pp. 447–453, 2015.

Pai Chet Ng is currently working toward the PhD degree in the Department of Electronic and Computer Engineering at the Hong Kong University of Science and Technology (HKUST) since 2015. She received her BS degree in Telecommunication Engineering from Multimedia University, Malaysia. She worked as research engineer prior to joining the HKUST-NIE Social Media Lab. Her research interests include cyber-physical system, mobile and IoT analytics.

James She is an assistant professor in the Department of Electronic and Computer Engineering at the Hong Kong University of Science and Technology (HKUST), and a visiting research fellow at the University of Cambridge. He is also the founding director of Asia's first social media lab, HKUST-NIE Social Media Lab, and spearheads multidisciplinary research and innovation in analytics and systems for social media and multimedia big data, smart/wearable device based interactive technologies in cyber-physical system or IoT infrastructure, and new media technologies and productions for art and culture. Since 2016, James became an associate editor for ACM Transaction on Multimedia Computing, Communications and Applications.

Soochang Park is a research associate at Hong Kong University of Science and Technology (HKUST). He worked in Institut Mines-Telecom, Telcom SudParis, France, as a research associate from 2013 to 2015, and was with Rutgers University, United States, as a postdoctoral researcher in 2012. He received his Ph.D. degree from Chungnam National University, Korea, in 2011. His research focuses on wireless networks, Internet of Things, and data analytics.